Plant Biotechnology Journal
Open Access

Plant Biotechnology Journal (2022) **20**, pp. 1042–1053 doi: 10.1111/pbi.13782

Dissection of the genetic architecture of peduncle vascular bundle-related traits in maize by a genome-wide association study

Gaoyang Sun[1,2], Xuehai Zhang[1,*], Haiyang Duan[1], Jionghao Gao[1], Na Li[1], Pingping Su[1], Huiling Xie[1], Weihua Li[1], Zhiyuan Fu[1], Yubi Huang[2,*] and Jihua Tang[1,*]

[1]*National Key Laboratory of Wheat and Maize Crop Science, College of Agronomy, Henan Agricultural University, Zhengzhou, China*
[2]*College of Agronomy, Sichuan Agricultural University, Chengdu, China*

Received 7 March 2020;
revised 20 December 2021;
accepted 17 January 2022.
**Correspondence* (Tel 86-0371-56990186; fax 86-0371-56990188; email xuehai85@126.com (X.Z.); Tel 86-028-86290872; fax 86-028-86290870; email yubihuang@sohu.com (Y.H.); Tel 86-0371-56990336; fax 86-0371-56990188; email tangjihua1@163.com (J.T.))

Keywords: maize, peduncle, vascular bundle, genome-wide association study, genetic loci.

Summary

The peduncle vascular system of maize is critical for the transport of photosynthetic products, nutrients, and water from the roots and leaves to the ear. Accordingly, it positively affects the grain yield. However, the genetic basis of peduncle vascular bundle (PVB)-related traits in maize remains unknown. Thus, 15 PVB-related traits of 386 maize inbred lines were investigated at three locations (Yongcheng, 17YC; Kaifeng, 20KF; and Yuanyang, 20YY). The repeatability for the 15 traits ranged from 35.53% to 92.13%. A genome-wide association study was performed and 69 non-redundant quantitative trait loci (QTL) were detected, including 9, 41, and 27 QTL identified at 17YC, 20KF, and 20YY, respectively. These QTL jointly explained 4.72% (SLL) to 37.30% (NSVB) of the phenotypic variation. Eight QTL were associated with the same trait at two locations. Furthermore, four pleiotropic QTL were identified. Moreover, one QTL (*qPVB44*), associated with NSVB_20KF, was co-localized with a previously reported locus related to kernel width, implying *qPVB44* may affect the kernel width by modulating the number of small vascular bundles. Examinations of the 69 QTL identified 348 candidate genes that were classified in five groups. Additionally, 26 known VB-related homologous genes (e.g. *VLN2*, *KNOX1*, and *UGT72B3*) were detected in 20 of the 69 QTL. A comparison of the NSVB between a *Zmvln2* EMS mutant and its wild type elucidated the function of the candidate gene *ZmVLN2*. These results are important for clarifying the genetic basis of PVB-related traits and may be useful for breeding new high-yielding maize cultivars.

Introduction

Maize plays an important role in ensuring global food security. In maize, the relative effects of the supply of assimilates and the capacity of the reproductive sink to accumulate assimilates on plant growth and kernel development remain controversial (Gambín *et al.*, 2006). Clarifying the key components (such as the source, sink, and flow) that determine the 'source–sink' relationships is important for maximizing maize yield (Borrás *et al.*, 2003, 2004). Although the 'source–sink' relationships have been reported in different plant species (Chang and Zhu, 2017), the vascular system, which linking the source and the sink, is poorly studied and also critical for understanding the 'flow' process.

The plant vascular system, which mediates the transport of materials and serves as an effective long-distance communication system, has been subjected to long-term selection pressure in terrestrial environments (Lucas *et al.*, 2013). A network of vascular bundles (VBs) connects all organs of gramineous plants, from the roots through the stems to the leaves as well as through the peduncles and ultimately to the grains (Zhai *et al.*, 2018). An individual VB in the stem transfers assimilates from a source leaf to a sink region and is an important conduit for water, mineral nutrients, and photosynthetic products (Peterson *et al.*, 1982). There is a significant positive correlation between VB-related traits and grain yield and its components (Evans *et al.*, 1970; Nátrová, 1991). In maize, because the peduncle is the only channel connecting the stem and the ear, it influences grain yield after ear ripening. Thus, elucidating the genetic basis of peduncle vascular bundle (PVB)-related traits in maize may provide useful information for breeding new high-yielding cultivars.

Substantial progress has been made in characterizing the development and function of the vascular system at the physiological, genetic, and molecular biological levels (Li *et al.*, 2018; Lucas *et al.*, 2013; Wang *et al.*, 2019). The early stage of VB development predominantly involves an adaptation to severe external environmental conditions (Franks and Brodribb, 2005; Ruszala *et al.*, 2011). Under favourable environmental conditions, wood grows rapidly and the anatomy and chemical composition of the culms differ from those that develop under drought stress (Lucas *et al.*, 2013). Regarding water-deficit stress, the 'source–flow–sink' relationship affects the seed set rate (Li *et al.*, 2018). Certain signalling molecules, such as auxin (Smetana *et al.*, 2019), jasmonate (Sehr *et al.*, 2010), abscisic acid (Campbell *et al.*, 2018), ethylene (Etchells *et al.*, 2012), and other small regulatory molecules, play crucial roles in VB morphogenesis. These plant growth regulators rarely act alone, and their signalling pathways are interconnected in complex networks. For example, auxin transport regulates VB development at different stages, but there is increasing evidence suggesting that

auxin functions coordinately with other growth regulators, including cytokinin and ethylene (Dettmer *et al*., 2009; Nagata *et al*., 2001; Yamamoto *et al*., 2001). Additionally, *MP*, *ARF7*, and *ARF19* are the key transcription factors (TFs) in the auxin signal transduction pathway, and high auxin levels can promote the expression of *HD-ZIP III*, *PXY*, and *WOX4* through these TFs in vascular cambium stem cell organizer cells (Smetana *et al*., 2019). Moreover, the NAC and MYB family TFs are critical regulators of lignin deposition in Arabidopsis secondary cell walls (SCWs) (Mitsuda *et al*., 2007; Zhou *et al*., 2009).

The rapid development of next-generation sequencing technologies and molecular marker genotyping techniques has enabled researchers to dissect the genetic basis of complex agronomic traits in plants via linkage analysis and genome-wide association study (GWAS) (Xiao *et al*., 2017). Many quantitative trait loci (QTL) for VB-related traits in C_3 species have been identified and several genes have been cloned (Terao *et al*., 2010; Wang *et al*., 2016). Compared with C_4 plants, it is easier to accurately determine the structure and phenotype of VBs in C_3 plants. In maize, which is a typical C_4 plant, the number of VBs varies among internodes (Shane *et al*., 2000). Assessing the phenotypic parameters for VB-related traits, especially for peduncle or PVB-related traits, is a major challenge in maize, and there has been relatively little research on the underlying genetic mechanism. Thus, the genetic basis of PVB-related traits must be investigated, and the PVB-associated genes in maize should be identified.

In the current study, using 0.56 M single nucleotide polymorphisms (SNPs), a GWAS method was conducted to investigate the natural allelic variations that contribute to PVB-related traits. The main purposes were as follows: (i) explore the distribution of PVB-related traits and (ii) to identify the SNPs/loci and candidate genes significantly associated with PVB-related traits in different environments. The results will enhance our understanding of the genetic mechanisms underlying PVB-related traits in maize and may be useful for breeding new high-yielding cultivars.

Results

Phenotypic assessment

Fifteen PVB-related traits of the association mapping population were examined at three locations (Figure 1, Table S1), namely Yongcheng (YC) in 2017 and Kaifeng (KF) and Yuanyang (YY) in 2020 (hereafter referred to as 17YC, 20KF, and 20YY, respectively). The traits varied considerably at all locations (Table 1, Figures S1 and S2). The largest and smallest variations were for ALVB_17YC (1.69–51.39 mm^2) and DEH_17YC (7.75–17.44 mm), respectively (Table 1). The absolute kurtosis and skewness of most PVB-related traits were <1, reflecting the normal distribution of the traits (Table 1, Figure S1), which were typical quantitative traits controlled by multiple genes with mostly minor effects.

A Pearson correlation analysis indicated that most traits were significantly correlated. The coefficients ranged from 0.88 (between TAVB_20KF and ALVB_20KF) to −0.39 (between DEH_20KF and TAVB_AOS_20KF; Figure 2). Most of the 15 PVB-related traits of the association mapping population varied significantly depending on the genotype, environment, and the genotype × environment interaction. Moreover, the repeatability of the 15 PVB-related traits ranged from 35.53% to 92.13% (Table S2).

Genome-wide association study

In the current study, 157 SNP–trait associations (involving 133 SNPs) were detected at a significance level of $-\log_{10}(P) \geq 5.4$ [$P \leq 1$/effective number (EN) = 3.93×10^{-6}; EN is 254 535] under the Q + K model (Table S3, Figure S3). The significant SNPs were located on all 10 chromosomes, with chromosomes 7 and 10 carrying the most (39) and fewest (4) SNPs, respectively (Figures 3 and 4, Table S3). According to the linkage disequilibrium (LD) decay of the association mapping population (Li *et al*., 2013), a QTL was defined as the 50-kb regions flanking each side of a significant SNP. Here, a total of 69 non-redundant QTL (the QTL with overlapping flanking intervals were categorized as a non-redundant QTL) were detected across 10 chromosomes (Figure 4, Table S3). Of these QTL, 69.6% and 30.4% were, respectively, major-effect ($R^2 \geq 10\%$) and minor-effect ($R^2 < 10\%$) QTL. These results, which were consistent with the genetic basis of quantitative traits, indicate that the VB traits are controlled by major-effect QTL and multiple QTL with minor effects. Specifically, at 17YC, 14 SNP–trait associations involved eight PVB-related traits (ALVB, ASVB, SLL, TAVB, TAVB_AOS, NLVB, NSVB, and TNVB). These SNPs were distributed in nine non-redundant QTL. The percentage of the variation explained by each QTL (i.e. R^2) ranged from 8.84% to 11.51%, with a mean of 10.05%. Four major-effect QTL that explained more than 10% of the phenotypic variation (R^2 = 10.03–11.51%) were identified. At 20KF, 88 SNP–trait associations involved 12 PVB-related traits (ALVB, ASVB, TAVB, AOS, ASLVB, ASSVB, LEH, LNEH, NLVB, TNVB, NSVB, and TAVB_AOS). These SNPs were located within 41 non-redundant QTL, which explained 8.63% to 14.09% (mean of 10.64%) of the phenotypic variation. At 20YY, 55 SNPs associated with nine PVB-related traits (ASVB, TAVB, AOS, ASLVB, ASSVB, LEH, LNEH, NLVB, and NSVB) were within 27 non-redundant QTL, which explained between 8.74% and 13.21% (mean of 10.55%) of the phenotypic variation (Table S3). The results indicated that the QTL identified for individual trait accounted for 8.84% (ALVB) – 15.01% (TAVB_AOS), 10.36% (ASSVB) – 42.75% (NLVB), and 8.74% (LNEH) – 36.25% (NLVB) of the phenotypic variation at 17YC, 20KF, and 20YY, respectively (Table 2). Additionally, according to the BLUP data for the three locations, the QTL for individual trait explained 4.72% (SLL) to 37.30% (NSVB) of the phenotypic variation (Table 2).

On the basis of the GWAS results and the annotated maize B73 RefGen_v2 genome assembly (https://www.maizegdb.org/gbrowse), candidate genes were detected in the 50-kb regions flanking significant loci. A total of 348 candidate genes were identified, of which 26 genes (Table S3, in bold and underlined), including *VLN2* (*GRMZM2G180988*), *CCoAOMT1* (*GRMZM2G033952* and *GRMZM2G332522*), and *MYB60* (*GRMZM2G172487*), were associated with VB-related traits. Details regarding the GWAS results, including the R^2 and *P*-values for each non-redundant QTL, the physical positions of SNPs, and the most likely candidate genes and their annotations, as well as the homologs of the candidate genes in Arabidopsis are listed in Table S3.

Common QTL were identified in different locations

Eight QTL (*qPVB6*, *qPVB15*, *qPVB28*, *qPVB32*, *qPVB40*, *qPVB42*, *qPVB45*, and *qPVB63*) were detected at two locations (Figure 4), of which two QTL (*qPVB6* and *qPVB32*) were associated with NLVB_20YY and NLVB_20KF, and three QTL (*qPVB15*, *qPVB40*,

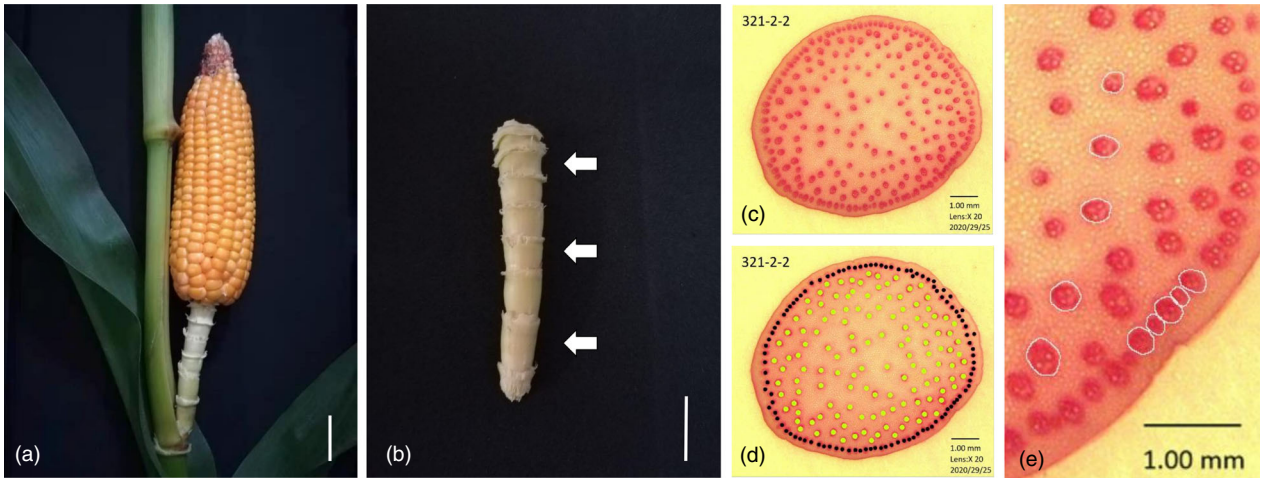

Figure 1 Transverse sectioning and phenotypic analysis of the maize peduncle. (a) Maize ear and peduncle. Scale bar, 1 cm. (b) Peduncle examined in this study. White arrows indicate the locations corresponding to the freehand-drawn sections. Scale bar, 1 cm. (c) Freehand-drawn transverse section of the peduncle. Scale bar, 1 mm. (d) The Sketchbook software on an iPad was used to count the number of vascular bundles (VBs). Black dots represent small VBs, whereas pale green dots represent large VBs. Scale bar, 1 mm. (e) The VB area was calculated using the CAD software. The mean area of adjacent VBs was recorded.

and *qPVB42*) were related to NSVB_20KF and NSVB_20YY. Additionally, *qPVB28* was associated with NLVB_17YC and NLVB_20YY, *qPVB45* was related to LEH_20KF and LEH_20YY, and *qPVB63* was associated with AOS_20KF and AOS_20YY (Figure 4). Furthermore, four pleiotropic QTL (*qPVB15* associated with TNVB_20KF, NSVB_20YY, and NSVB_20KF; *qPVB17* related to ALVB_20KF and TAVB_20KF; *qPVB28* associated with NLVB_17YC, ASVB_20YY, and NLVB_20YY; and *qPVB35* related to ASVB_20KF and TAVB_20KF) were detected. The co-localized and pleiotropic QTL were significantly associated with PVB-related traits and accounted for 8.49–13.53% of the phenotypic variation. Interestingly, one non-redundant QTL (*qPVB44*) overlapped a previously reported locus associated with kernel width (KW) (Yang *et al*., 2014). This QTL was on chromosome 7 and was associated with the number of small VBs (NSVB) at 20KF. Moreover, it explained 10.75% of the phenotypic variation (Table S3).

Candidate gene analysis

In this study, 556 809 polymorphisms with a minor allele frequency (MAF) ≥ 0.05 were selected for a GWAS, and 69 non-redundant QTL were identified. The QTL contained 348 candidate genes, with 1–12 candidate genes (mean of 5.0) predicted for each QTL. The candidate genes were functionally annotated using online resources (https://www.maizegdb.org/ and https://www.ncbi.nlm.nih.gov/) and divided into five groups (Figure S4). The first group included 26 genes, of which seven encode MYB and NAC family TFs involved in regulating lignin deposition in Arabidopsis SCWs (Mitsuda *et al*., 2007; Zhou *et al*., 2009). Additionally, *ANAC002* (i.e. homolog of *GRMZM2G014653*) is a salt and drought stress-responsive gene potentially targeted by ERF139, which coordinates xylem cell expansion and SCW deposition (Wessels *et al*., 2019). Two genes (*GRMZM2G052365* and *GRMZM2G020986*) were revealed as modulators of cell wall compositions. Another two genes (*GRMZM2G332522* and *GRMZM2G033952*), which were associated with NLVB_20KF, were homologous to the Arabidopsis gene (*CCoAOMT1*) encoding a key enzyme involved in lignin polymerization and synthesis (Endo *et al*., 2019). The Arabidopsis homolog of *GRMZM2G159431* was identified as *KNAT7*, which has recently been implicated in the direct regulation of xylan biosynthesis genes affecting the SCW and seed coat mucilage of Arabidopsis (He *et al*., 2018; Wang *et al*., 2020).

Although there were 121 and 20 genes in the second and third groups, respectively, none of them were VB-related genes or homologs of previously reported genes affecting VBs. Most of the genes in the fourth group (169/348) were related to biosynthesis, metabolism, cell division, and growth. For example, *GRMZM2G074356* and *GRMZM2G074404* encode Bax inhibitor-1 family proteins, whereas *GRMZM2G405185* encodes AtGCP3-interacting protein 1. The genes in the second, third, and fourth groups may not be directly involved in pathways mediating VB development, and the polymorphic markers may be linked to a neighboring gene (Li *et al*., 2013).

The fifth group was characterized by genes involved in signal transduction (12/348), including seven signalling pathway genes (*GRMZM2G473906*, *GRMZM2G114192*, *GRMZM2G148807*, *GRMZM2G067555*, *GRMZM2G100579*, *GRMZM2G109472*, and *GRMZM2G157760*), four electron transfer pathway genes (*GRMZM2G114739*, *GRMZM2G039278*, *GRMZM5G877259*, and *AC209987.4_FG002*), and a BR-signalling kinase gene (*GRMZM2G127050*). The identification of these genes provides a foundation for further analyses of the genetic basis of PVB-related traits and confirms the utility of GWAS-based analyses of complex agronomic traits.

Functional verification of the candidate gene *ZmVLN2*

The lead SNP (chr8.S_158118795) in *qPVB55* on chromosome 8 was associated with NSVB_17YC and was detected 18.3 kb upstream of *GRMZM2G180988* (Figure 5a,b). The Arabidopsis homolog of *GRMZM2G180988* is *VLN2*, which encodes a protein that functions redundantly with VLN3 to modulate sclerenchyma development and directional organ growth via the bundling of actin filaments (Bao *et al*., 2012; Honing *et al*., 2012). In rice, *VLN2* regulates the plant architecture (e.g. the size of root VBs) by affecting microfilament dynamics and auxin transport (Wu *et al*.,

Table 1 Descriptive statistics for the peduncle vascular bundle-related traits of 386 maize inbred lines grown at three locations

Location	Trait*	Unit	Range	Mean ± SD†	Skew‡	Kurt§
2017	LEH	Mm	48.59–259.63	118.16 ± 41.06	0.83	0.43
Yongcheng (17YC)	DEH	Mm	7.75–17.44	12.35 ± 1.87	−0.02	0.02
	LNEH	Count	5.00–11.33	8.17 ± 1.33	0.03	−0.63
	SLL	Mm	6.06–25.24	14.32 ± 4.22	0.39	−0.60
	NLVB	Count	70.00–333.33	150.84 ± 38.29	0.83	1.91
	NSVB	Count	71.67–233.83	148.45 ± 33.63	0.47	−0.03
	TNVB	Count	148.00–752.50	307.97 ± 77.18	1.25	4.30
	ASLVB	mm^2	0.04–0.26	0.10 ± 0.04	1.38	2.04
	ASSVB	mm^2	0.02–0.16	0.06 ± 0.02	1.28	1.91
	AOS	mm^2	44.23–300.26	135.54 ± 56.33	0.78	−0.05
	ALVB	mm^2	1.69–51.39	14.91 ± 7.52	1.74	4.26
	ASVB	mm^2	2.66–19.99	8.38 ± 3.50	1.01	0.89
	TAVB	mm^2	8.12–49.57	22.48 ± 8.75	0.95	0.60
	DVB	Count	0.80–5.20	2.71 ± 0.92	0.42	−0.34
	TAVB_AOS	Count	0.07–0.44	0.19 ± 0.05	1.15	2.77
2020	LEH	Mm	27.30–172.57	81.37 ± 26.38	0.66	0.64
Kaifeng (20KF)	DEH	Mm	5.76–18.44	11.89 ± 2.20	0.29	0.09
	LNEH	Count	4.00–11.00	7.36 ± 1.24	0.17	0.08
	SLL	Mm	3.94–21.73	11.18 ± 3.37	0.45	−0.27
	NLVB	Count	80.33–262.94	148.46 ± 36.91	0.77	0.16
	NSVB	Count	86.78–368.00	169.68 ± 54.00	1.03	1.03
	TNVB	Count	174.67–527.50	314.25 ± 74.78	0.63	0.03
	ASLVB	mm^2	0.04–0.20	0.09 ± 0.03	1.18	2.90
	ASSVB	mm^2	0.02–0.10	0.05 ± 0.02	0.70	0.39
	AOS	mm^2	33.41–195.31	89.36 ± 30.24	0.70	0.40
	ALVB	mm^2	5.22–25.83	12.66 ± 4.32	0.68	−0.07
	ASVB	mm^2	2.42–17.57	7.93 ± 2.97	0.87	0.77
	TAVB	mm^2	8.73–42.22	20.74 ± 6.80	0.66	0.17
	DVB	Count	1.40–6.70	3.67 ± 1.10	0.41	−0.36
	TAVB_AOS	Count	0.12–0.37	0.23 ± 0.05	0.37	−0.36
2020	LEH	Mm	30.49–174.35	83.02 ± 26.98	0.88	0.79
Yuanyang (20YY)	DEH	Mm	7.18–18.04	11.65 ± 1.99	0.45	0.28
	LNEH	Count	4.00–10.67	7.64 ± 1.16	0.07	−0.11
	SLL	Mm	4.36–18.96	10.83 ± 2.95	0.60	−0.10
	NLVB	Count	75.11–307.56	155.34 ± 36.62	0.71	0.72
	NSVB	Count	84.67–372.00	170.40 ± 57.19	1.09	0.77
	TNVB	Count	170.00–521.44	317.59 ± 72.56	0.45	−0.24
	ASLVB	mm^2	0.04–0.18	0.09 ± 0.02	0.69	0.67
	ASSVB	mm^2	0.02–0.12	0.05 ± 0.02	0.77	0.49
	AOS	mm^2	34.28–223.91	90.02 ± 31.54	1.09	1.83
	ALVB	mm^2	5.76–28.66	14.40 ± 5.28	0.64	−0.20
	ASVB	mm^2	3.48–20.82	8.93 ± 3.71	0.84	0.20
	TAVB	mm^2	10.40–56.44	24.07 ± 9.40	0.93	0.54
	DVB	Count	1.37–8.17	3.87 ± 1.24	0.75	0.81
	TAVB_AOS	Count	0.13–0.55	0.27 ± 0.08	0.86	0.69

*Abbreviations and units for each trait are listed in Table S1.

†Standard deviation.

‡Skewness, which reflects the asymmetry of the probability distribution of a real-valued random variable about its mean.

§Kurtosis, which reflects the 'tailedness' of the probability distribution of a real-valued random variable.

2015). In maize, *VLN2* may influence cytoskeleton organization, but this possibility remains to be experimentally verified. We designated *GRMZM2G180988* in maize as *ZmVLN2*. To functionally characterize *ZmVLN2*, a B73 ethyl methane sulfonate (EMS) mutant (Mut_Sample: EMS4-0afc18) with a termination mutation in the seventh exon was obtained from a maize EMS mutant library (http://www.elabcaas.cn/memd/) (Figure 5d). A comparison of the PVB-related traits of the *Zmvln2* mutant and the *ZmVLN2* wild-type revealed the *Zmvln2* mutant had a significantly smaller peduncle diameter, but there were no significant differences in LEH and LNEH (Figure 5e). We also detected significant decreases in NSVB, AOS, TAVB, ASVB, ALVB, ASLVB, and TNVB in the mutant, relative to the corresponding wild-type values (Figure 5f–i). These results suggested that

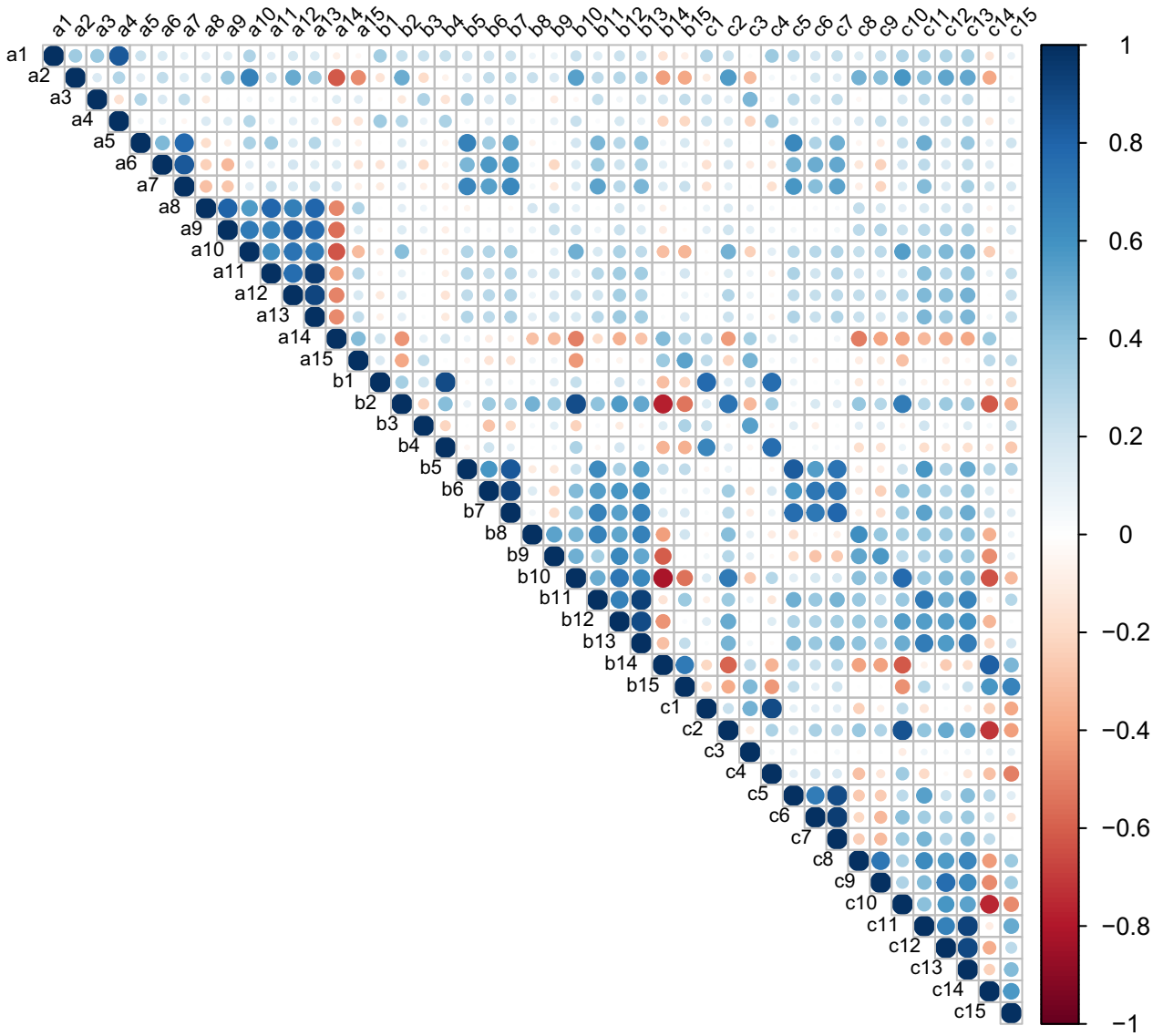

Figure 2 Correlation coefficients for peduncle vascular bundle-related traits in the maize association mapping population at three locations. a, b, and c refer to Yongcheng in 2017, Kaifeng in 2020, and Yuanyang in 2020, respectively. 1–15 refer to LEH, DEH, LNEH, SLL, NLVB, NSVB, TNVB, ASLVB, ASSVB, AOS, ALVB, ASVB, TAVB, DVB, and TAVB_AOS, respectively.

ZmVLN2 is the candidate gene in *qPVB55* that affects maize VB development.

Haplotype analysis of *ZmVLN2*

To investigate the *ZmVLN2* haplotype, the LD between the lead SNP and all polymorphic sites in *ZmVLN2* was estimated. The results revealed the substantial LD between the lead SNP chr8.S_158118795 (P_{MLM} = 3.01e-07) and nearly half of the polymorphic sites in *ZmVLN2* (Figure 5c). The subsequent analysis of 15 SNPs (MAF ≥ 0.05) in *ZmVLN2* among the 287 maize inbred lines at 17YC detected 19 haplotypes, with most lines (244) belonging to Hap1, Hap2, Hap3, and Hap4 (Table S4). More specifically, 223 lines belonged to Hap1 and Hap2. Regarding the NSVB, there were highly significant differences between Hap1 and Hap2 (P = 3.02e-07) as well as between Hap2 and Hap4 (P = 4.70e-03), but there was no significant difference between Hap2 and Hap3 (Figure S5). We also analyzed the remaining 14 PVB-related traits. The results for seven of these traits (DEH, NLVB, TNVB, ALVB, ASVB, TAVB, and AOS) were consistent with those of NSVB (Figure S5). The distribution of the inbred lines from temperate and tropical/sub-tropical regions or derived from specific breeding materials among the four haplotypes indicated that most of the maize inbred lines in China belonged to Hap2 (29/44) (Table S5). Considered together, these findings suggest that natural variations in *ZmVLN2* affect the NSVB and seven other PVB-related traits, which may have been influenced by selection pressures during breeding.

Discussion

Vascular bundles are conduits for water and nutrients, while also providing mechanical support for plant growth. Several researchers have recently focused on VB-related traits (Li *et al.*, 2018; Lucas *et al.*, 2013; Wang *et al.*, 2019). Huang *et al.* (2016)

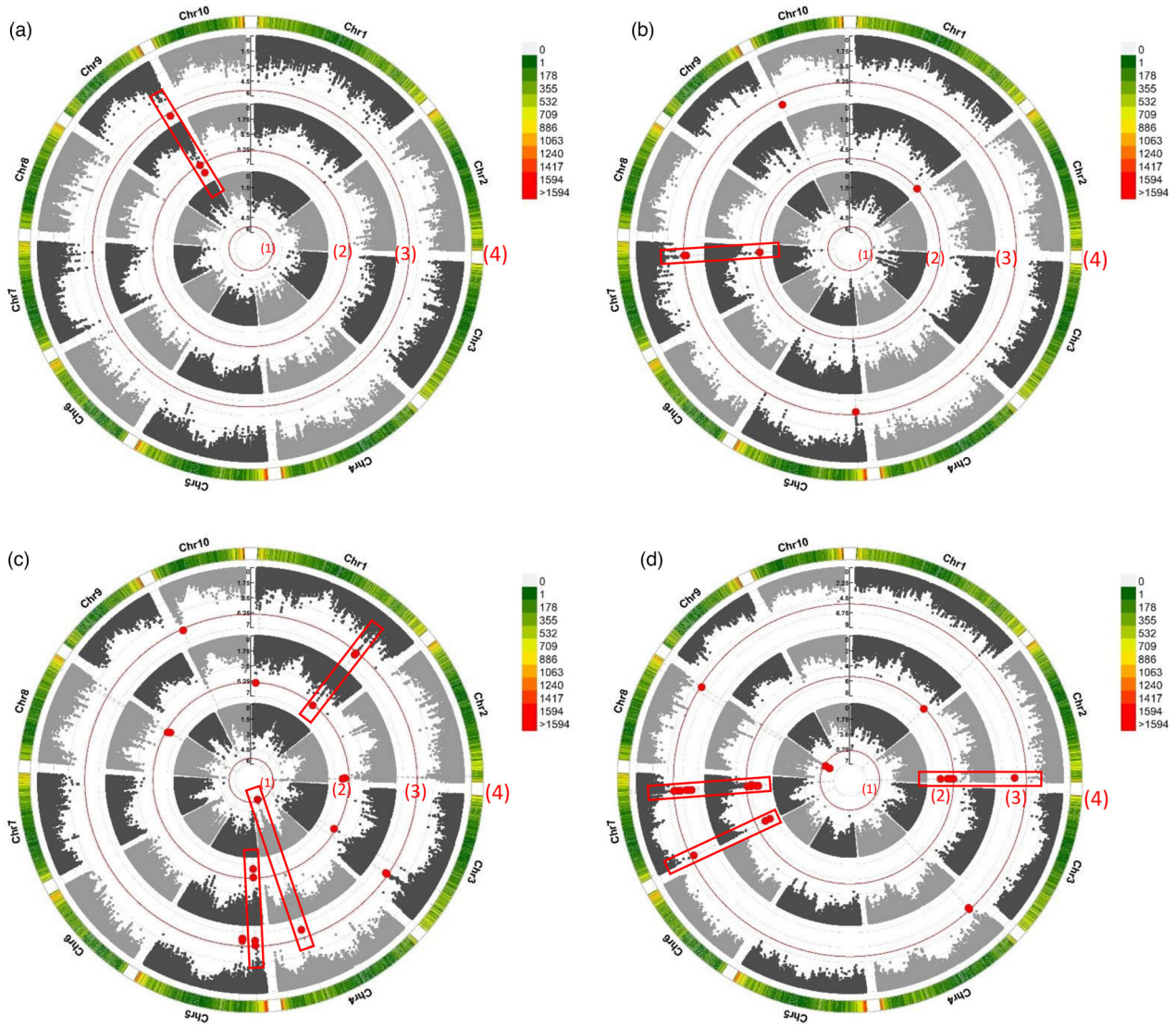

Figure 3 Manhattan plots of the association analysis of AOS, LEH, NLVB, and NSVB at three locations. a, b, c, and d represent AOS, LEH, NLVB, and NSVB, respectively. The red line indicates the significance threshold ($P = 3.93 \times 10^{-6}$). Significant SNPs are indicated by red dots. (1) – (3) represent different locations: (1), 2017 Yongcheng; (2), 2020 Kaifeng; (3), 2020 Yuanyang. (4) indicates the distribution of SNPs on 10 chromosomes in the association mapping population. The colour represents SNP marker density. Stable SNPs detected at different locations are indicated by red rectangular boxes.

constructed a recombinant inbred population comprising 866 lines derived from a cross between inbred lines of a natural accession of teosinte (*Zea mays* subsp. *parviglumis*) and the maize inbred line W22. They identified one QTL (*qVb9-2*) within the 114.8–127.5 Mb interval on chromosome 9, which was significantly associated with the TNVB in the uppermost portion of the stem. Zhai *et al*. (2018) conducted a GWAS of 423 rice accessions and identified 48 QTL for PVB-related traits. The maize peduncle is typically composed of multiple nodes and, as a stem branch, provides an important bridge connecting the stem and the ear. It is also the only channel for the transport of assimilates and water to the grain. However, not all VBs can reach adjacent internodes through the stem nodes (Shane *et al*., 2000). Moreover, the number and size of VBs vary among internodes, and the phenotypic characteristics of PVB-related traits are not easily evaluated. To date, relatively little research has been conducted on the genetic regulation of PVB-related traits in maize.

In the present study, 45 variables (i.e. 15 PVB-related traits at three locations) were included in a GWAS. We identified 157 significant SNP–trait associations, which involved 69 non-redundant QTL that explained 8.49%–14.09% of the phenotypic variation. Eight non-redundant QTL (*qPVB6*, *qPVB15*, *qPVB28*, *qPVB32*, *qPVB40*, *qPVB42*, *qPVB45*, and *qPVB63*) were detected at two study locations. Notably, five of these QTL (*qPVB15*, *qPVB32*, *qPVB42*, *qPVB45*, and *qPVB63*) explained more than 10% of the phenotypic variation at the two locations. Specifically, *qPVB15*, *qPVB32*, *qPVB42*, *qPVB45*, and *qPVB63*, respectively, explained 12.20%, 12.58%, 11.52%, 10.05%, and 12.62% of the phenotypic variation at 20KF as well as 11.96%, 10.55%, 13.53%, 10.39%, and 11.10% of the phenotypic variation at 20YY. Therefore, these QTL provide important information regarding the genetic mechanism underlying PVB-related traits and should be considered for future fine-mapping and molecular breeding. Moreover, 88.41% (61/69) of the non-redundant QTL

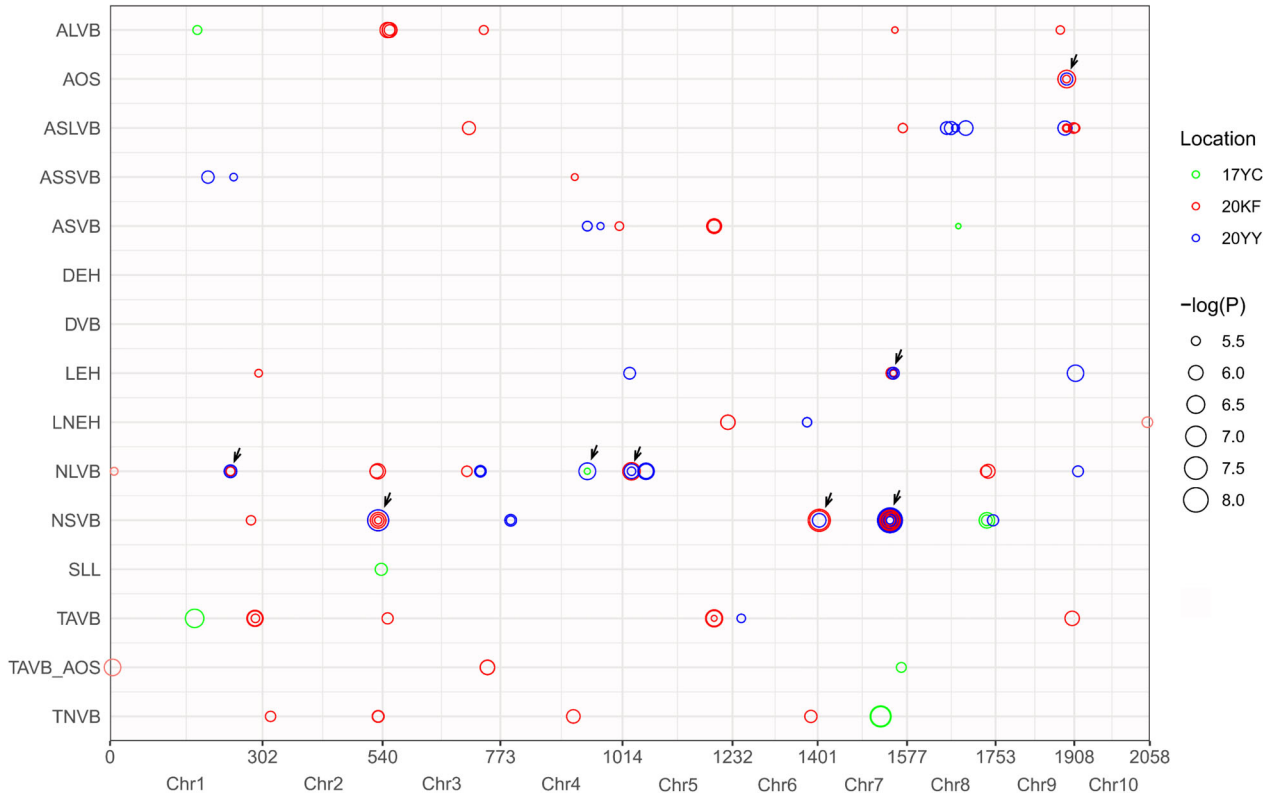

Figure 4 Chromosomal distribution of PVB-associated QTL detected in the maize association mapping population. The QTL position and significance (reflected by circle size) across the maize genome are presented. The x-axis indicates the physical positions in the maize genome (in Mb). Details regarding the QTL are provided in Table S3. The study locations are differentiated by colour. The QTL detected at two locations are marked by a black arrow.

Table 2 Total phenotypic variation explained by the QTL identified for PVB-related traits at 17YC, 20KF, and 20YY

	QTL Num.				PVE (%)			
Trait	17YC	20KF	20YY	BLUP*	17YC	20KF	20YY	BLUP*
LEH	0	3	3	5	NA	19.78	25.76	17.04
DEH	0	0	0	0	NA	NA	NA	NA
LNEH	0	2	1	3	NA	26.17	8.74	14.80
SLL	1	0	0	1	10.03	NA	NA	4.72
NLVB	1	8	8	15	9.22	42.75	36.25	25.46
NSVB	1	5	5	9	10.72	41.53	34.52	37.30
TNVB	1	4	0	5	11.28	23.04	NA	15.41
ASLVB	0	6	5	11	NA	39.03	29.92	23.40
ASSVB	0	1	2	3	NA	10.36	11.58	7.13
ALVB	1	5	0	6	8.84	27.89	NA	9.39
ASVB	1	2	2	5	9.11	16.15	18.74	14.32
TAVB	1	5	1	7	11.51	36.99	9.55	19.71
AOS	0	2	1	2	NA	24.11	11.10	8.38
DVB	0	0	0	0	NA	NA	NA	NA
TAVB_AOS	2	1	0	3	15.01	14.09	NA	13.57

NA, no QTL was detected; Num., number; PVE, phenotypic variation explained.
*A combination of the 17YC, 20KF, and 20YY locations.

were identified at only one location; others are stable across locations (Table S3). There are two possible explanations for this finding that individual QTL appear to show a range of sensitivities to environment. First, the examined traits are quantitative traits that controlled by multiple genes with minor effects are considerably more influenced by environmental conditions (Paterson *et al.*, 1991); second, affected by phenotypic plasticity that QTL effect values vary in different environments (Liu *et al.*, 2021).

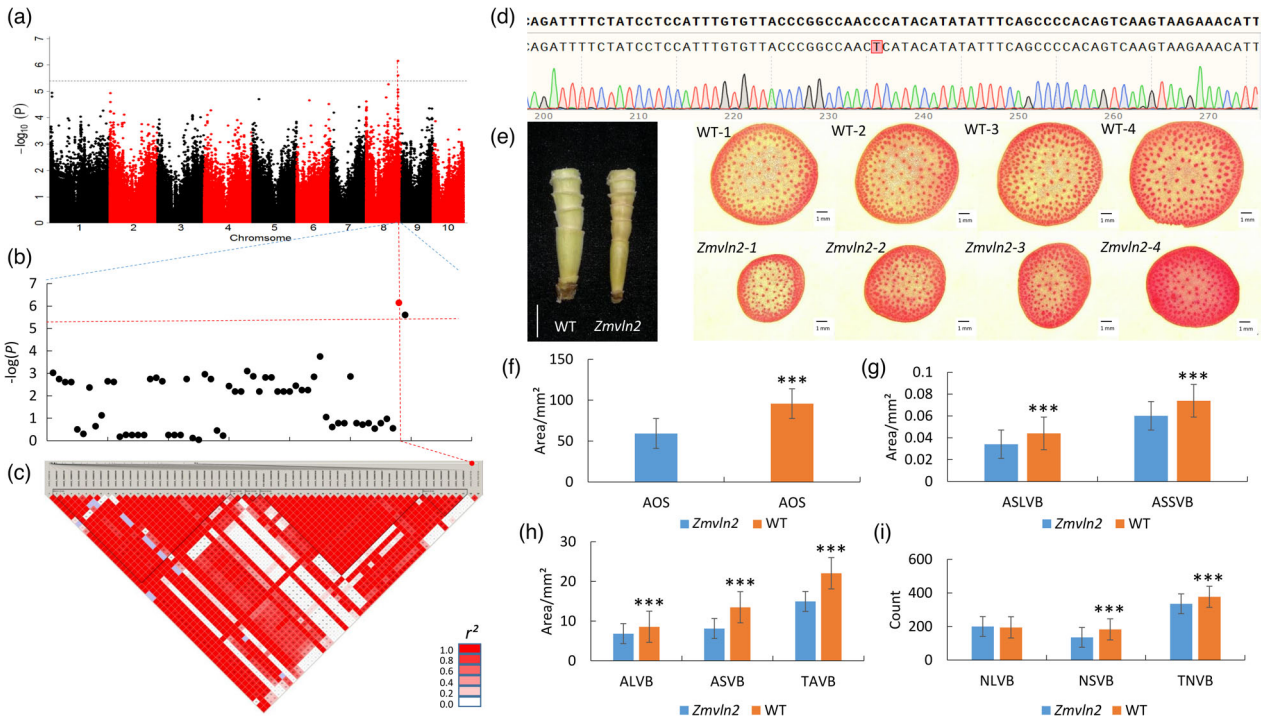

Figure 5 A mutated *ZmVLN2*, which is a candidate gene in *qPVB55*, affects several PVB-related traits. (a) Manhattan plot of the number of small vascular bundles (NSVB) at Yongcheng in 2017. The black dotted line represents the threshold $-\log_{10}(P) \geq 5.4$ ($P \leq 3.93 \times 10^{-6}$). (b) Enlarged Manhattan plot of the lead SNP and 57 SNPs within *ZmVLN2*. The red plot represents the lead SNP. (c) Pairwise r^2 values (a measure of LD) for all polymorphic sites in *ZmVLN2*; the colour intensity represents the degree of genetic linkage. Black and bold lines represent genes. The lead SNP was detected 18.3 kb upstream of *ZmVLN2*. (d) A homozygous *Zmvln2* mutant was obtained following an EMS treatment. (e) Phenotypic comparison between the homozygous *ZmVLN2* wild-type (WT) control and the *Zmvln2* mutant. Scale bar, 1 cm. (f–i) Significance of the differences in the PVB-related traits between the WT and *Zmvln2* mutant plants ($n \geq 3$). Data are presented as the mean ± standard deviation. $^{***}P < 0.001$ denotes a significant difference between the WT and *Zmvln2* plants.

On the basis of the B73 reference genome sequence, 348 candidate genes were identified within the 69 non-redundant QTL. The candidate genes were distributed in five groups according to their functions. Most of the genes in the first group are involved in the production of plant vascular tissue components (Table S3). For example, the homolog of *GRMZM2G372068* is *UGT72B3*. Both *UGT72B3* and *UGT72B1* encode glucosyltransferases, and *UGT72B1* is highly expressed in young stem tissues, especially xylem tissues (Lin *et al*., 2016). The homolog of *GRMZM2G386971* in Arabidopsis is *GAUT1*. A previous study demonstrated that *GAUT1* and *GAUT7* encode core parts of a plant cell wall pectin biosynthesis-related homogalacturonan: galacturonosyltransferase complex (Atmodjo *et al*., 2011). The homolog of *GRMZM2G135195* was identified as *GAUT4*, which contributes to the biosynthesis of the pectin and xylan in cell walls and seed testa (Caffall *et al*., 2009). Another study indicated that *GRMZM2G113245* encodes a glycosyltransferase (F8H) that is a functional paralog of FRA8, which is involved in glucuronoxylan biosynthesis in Arabidopsis (Lee *et al*., 2009). In maize, *GRMZM2G038401* (*ndl1*) causes severe reproductive defects and is closely related to known genes associated with the regulation of the plant hormone auxin (Liu *et al*., 2019). Earlier research revealed *SMO2-2*, which is a homolog of *GRMZM2G176301*, helps maintain ideal sterol compositions partly through its effects on auxin accumulation, auxin response, and *PIN1* expression, thereby regulating Arabidopsis embryogenesis and postembryonic development (Zhang *et al*., 2016).

To explore the relationship between PVB-related traits and maize yield, the BLUP values of the yield and yield-related traits, including ear length (EL), ear diameter (ED), kernel length (KL), KW, kernel thickness (KT), and 100-grain weight (HGW), of 268 lines were obtained from an online source (http://www.maizego.org/Resources.html) (Yang *et al*., 2014) and used to perform a Pearson correlation analysis involving the PVB-related traits of the inbred lines at two locations (KF and YY). We determined that NSVB, NLVB, TNVB, ASLVB, DEH, ASVB, ALVB, and TAVB were positively correlated with ED, but LNEH was negatively correlated with ED. Both KL and KT were positively correlated with ALVB and TAVB, but KT was also positively correlated with ASLVB. Furthermore, ASVB, ALVB, and TAVB were positively correlated with HGW (Figure S6). Among the 69 non-redundant QTL, one (*qPVB44*) was associated with KW (Yang *et al*., 2014) and NSVB_20KF, implying that it may affect KW by regulating NSVB to increase the grain yield. Additionally, three candidate genes (*GRMZM2G111309*, *GRMZM2G413044*, and *GRMZM2G413030*) were detected within *qPVB44*. The Arabidopsis homolog of *GRMZM2G413044* is *XTH32*, which is primarily involved in the cellular glucan metabolic process that affects the cell wall. This finding is important for future studies on the relationship between NSVB and maize yield.

Ear-related traits, such as EL, ear row number (ERN), ear weight (EW), cob weight (CW), cob length (CL) and cob diameter (CD), are important factors influencing maize yield (Yang *et al*., 2014). Xiao *et al*. (2016) used a ROAM population consisting of 10 recombinant inbred lines to dissect the genetic basis of EL, ERN,

EW, and CW via separate linkage mapping (SLM), joint linkage mapping (JLM), and a GWAS, which resulted in the identification of many QTL. More specifically, 28, 5, and 2 of the QTL identified in the current study were also detected on the basis of the SLM, JLM, and GWAS results, respectively (Tables S6–S8). Moreover, 10 QTL associated with the ERN, CL, and CD of a NAM population (Brown *et al*., 2011) were among the QTL identified in our study (Table S9). Interestingly, *qPVB1* was identified by the SLM, JLM, and GWAS conducted in previous investigations (Brown *et al*., 2011; Xiao *et al*., 2016; Tables S6–S9). The homolog of *GRMZM2G159431* (in *qPVB1*) is *KNAT7*, whose function has already been mentioned in 'candidate gene analysis' section. Of the 36 QTL detected in more than one study, 13 (*qPVB6*, *qPVB8*, *qPVB25*, *qPVB30*, *qPVB36*, *qPVB41*, *qPVB56*, *qPVB60*, *qPVB61*, *qPVB62*, *qPVB63*, *qPVB65*, and *qPVB68*) were significantly associated with EW (Tables S6–S9), suggesting that these QTL may affect EL, ERN, EW, and CD by modulating TAVB_AOS, TNVB, and LEH, and ultimately influencing maize yield. Improving PVB-related traits, such as NSVB, TAVB_AOS, LEH, and TNVB, through breeding may lead to the development of new high-yielding maize cultivars.

Methods

Plant materials and field trials

A total of 386 maize inbred lines in the association mapping panel (AMP) were studied at three different locations in two years. In 2017, 287 of 386 maize inbred lines were grown at Yongcheng (17YC; 33°55′N, 116°26′E; Table S10), with an average temperature of 24.77 °C from June to October. In 2020, 272 of 386 inbred lines were grown at Kaifeng (20KF; 34°79′N, 114°35′E; Table S10) and Yuanyang (20YY; 35°03′N, 113°56′E; Table S10), with average temperatures of 23.10 and 22.60 °C, respectively, from June to October. In specific, 173 inbred lines were present in all three environments (17YC, 20KF, and 20YY); 99 unique inbred lines were planted at 20KF and 20YY, and 114 inbred lines were only planted at 17YC. At each location, the maize inbred lines were cultivated according to a randomized complete block design, with three replications. Plots consisted of 2-m rows that were separated by 0.22 m. The plants within each row were separated by 0.67 m. All inbred lines were from a subset of 513 maize lines that have been widely used for research (Xiao *et al*., 2017).

Sample processing, phenotyping, and statistical analyses

Peduncles were collected from plants to ensure the same parts were analyzed. Specifically, at 30 days after pollination, peduncles were collected from the uppermost ear of the maize inbred lines at three locations (Figure 1a). For each peduncle, the upper and lower internodes (i.e. the second internode from the top and bottom of the peduncle, respectively) as well as the middle internode (intermediate position) were examined. Thus, the first and last internodes of the peduncles were not included in this study (Figure 1b). The phenotypic data of each internode were recorded, after which the mean values for the three internodes were calculated and used for further analyses. Specifically, the samples were fixed in a solution comprising 38% formaldehyde, glacial acetic acid, and 70% alcohol (1:1:18, v/v/v). The peduncles were placed in 50-ml centrifuge tubes. Sufficient fixative solution was added to ensure the peduncles were submerged. The transparency agent and reservoir sealing agent were added and then the tubes were sealed and incubated at 4 °C.

The peduncles were removed from the fixative solution and then washed sequentially with 50%, 75%, and 100% alcohol and dried. A Vernier caliper was used to measure the LEH, DEH, and SLL. For the inbred lines at each location, the upper, middle, and lower peduncle internodes were examined regarding the NLVB, NSVB, TNVB, and AOS. For each internode, transverse sections were prepared (Figure 1a,b). The sections were fixed with 5% *m*-trihydroxybenzene and stained with concentrated hydrochloric acid. The stained sections were examined using the VHX-600 digital microscope (Keyence, Osaka, Japan; Figure 1c, d). The NLVB, NSVB, and TNVB data were recorded as previously described (Huang *et al*., 2016). Additionally, AOS, ASLVB, and ASSVB (five continuous measurements) were analyzed using the CAD software (version 2019) (Figure 1e).

The IBM SPSS Statistics software (version 19.0) was used for a two-way analysis of variance (ANOVA) and a Pearson correlation analysis of the PVB-related traits and the BLUP data for yield and the related traits (i.e. HGW, KL, KW, KT, EL, and ED; Yang *et al*., 2014). The general statistical analysis of all PVB-related traits (i.e. maximum, minimum, average, skewness, and kurtosis) was performed using Microsoft Excel 2013. The frequency distribution was plotted using the R program, and the repeatability (w^2) was calculated using the lmer function in the lme4 package of the R program (version 3.1.3; R Core Team, 2020; http://www.r-project.org/). The w^2 values for each PVB-related trait at three locations were calculated using the following formula as previously described (Knapp, 1986):

$$w^2 = \sigma_G^2/[\sigma_G^2 + (\sigma_{GE}^2/n) + \sigma_e^2/(nr)],$$

where n is the number of locations, r is the number of replications, and σ_G^2, σ_{GE}^2, and σ_e^2 represent the genotypic variance, the genotype × environment variance, and the error variance, respectively.

In this study, we treated each trait, location (YC, KF, and YY), and year (2017 and 2020) as individual variables for the GWAS. For example, TNVB_17YC represents the total number of VBs at Yongcheng in 2017. For each trait, the mean value for five plants at each location was used for the GWAS analysis. We recorded data for 45 variables (15 PVB-related traits at three locations) for the association mapping population consisting of 386 diverse inbred lines.

Genome-wide association study

Genotypic data for the inbred lines were generated in a previous study (Yang *et al*., 2014). Briefly, 513 maize inbred lines were genotyped using the Illumina Maize SNP50 BeadChip containing 56 110 SNPs (Li *et al*., 2013). Additionally, an RNA sequencing analysis of the developing maize kernels of 368 inbred lines (a subset of 513 lines) was performed at 15 days after pollination. Genotypic data (556 809 SNPs) from the two genotyping platforms were combined (Fu *et al*., 2013; Li *et al*., 2013). Following a two-step approach developed on the basis of an identity by descent-based projection and the *k*-nearest neighbor algorithm, 556 809 high-density SNP markers for the remaining 145 lines were obtained (Yang *et al*., 2014). This procedure resulted in 556 809 high-density SNPs (0.56 M SNPs, MAF ≥ 0.05) for the 513 inbred lines included in the GWAS. The SNP data are available online (http://www.maizego.org/Resources.html). The GWAS was conducted for all PVB-related traits at all three locations (17YC, 20KF, and 20YY). The Q + K model (accounting for both the Q and K matrices) involved a

compressed mixed linear model (cMLM) was used for perform GWAS in the TASSEL 3.0 software (Bradbury *et al.*, 2007). To determine the significance of the SNP–trait associations, we considered LD to be common among SNP pairs, and the effective number of independent SNP markers was calculated using the GEC tool (Li *et al.*, 2012). The number of independent markers suggested by the GEC tool was used to determine the global *P* threshold (*P* = 1/effective number of independent markers) and to minimize the number of genome-wide type I errors. The *P*-value of each SNP obtained from TASSEL 3.0 was used to generate QQ and Manhattan plots for all PVB-related traits. Moreover, combined with the genotypic information for all significant loci, the R function 'LM' was used to estimate the total contributions to the phenotypic variation.

Analysis of candidate genes

On the basis of the maize B73 genome assembly (B73 RefGen_v2), all candidate genes were downloaded and annotated using the MaizeGDB database (https://www.maizegdb.org/gbrowse) and InterProScan (http://www.ebi.ac.uk/interpro/). In a previous study, the LD of the association mapping population was estimated using 0.55 M SNPs, and the LD decay was 50 kb (r^2 = 0.1) (Li *et al.*, 2013). We annotated all candidate genes in a 100-kb region (50 kb upstream and downstream) surrounding the peak SNP, which is the SNP with the lowest *P*-value, of the identified significant QTL (Table S3). For QTL lacking appropriate candidates, the gene nearest the peak SNP was selected and annotated. The physical locations of the SNPs were determined according to B73 RefGen_v2. The candidate genes associated with VB-related traits were identified by searching for annotated Arabidopsis homologs with functions influencing VB traits in the MaizeGDB (https://www.maizegdb.org/) and NCBI (https://www.ncbi.nlm.nih.gov/) databases. For example, in Arabidopsis, NAC and MYB TFs are key regulators of lignin deposition in SCWs (Mitsuda *et al.*, 2007; Zhou *et al.*, 2009). Furthermore, some genes may indirectly affect VB development (e.g. *VLN2*; Bao *et al.*, 2012; Honing *et al.*, 2012; Wu *et al.*, 2015). Accordingly, the genes encoding NAC and MYB TFs and proteins that indirectly affect VBs may influence PVB development in maize.

Linkage disequilibrium and haplotype analyses

The LD was estimated by the squared allele frequency correlations of SNP pairs, which were calculated using the TASSEL 3.0 software. The LD plot was generated using Haploview 4.2. The LD was indicated using r^2 values for the SNP pairs multiplied by 100 (white, $r^2 = 0$; pale red, $0 < r^2 < 1$; red, $r^2 = 1$) (Barrett, 2009; Gabriel *et al.*, 2002). The haplotypes were classified on the basis of all SNPs (MAF $\geq$ 0.05) within a given target gene. The haplotypes that were present in at least 10 inbred lines were used for a comparative analysis (Table S4).

Genotyping of the EMS mutant *Zmvln2*

The EMS mutant *Zmvln2* (Mut_Sample: EMS4-0afc18) was obtained from the Maize EMS-induced Mutant Database (http://www.elabcaas.cn/memd/). To obtain mutants and wild-type lines with similar genetic background. The seeds were planted to produce F_1 seeds by self-pollination. And the plants containing heterozygous genotype in F_1 were selected to obtain F_3 seeds by self-pollination for two generations. In F_3 plants, the plants with homozygous wide-type *ZmVLN2* (WT) and EMS homozygous mutant *Zmvln2* (thereafter *Zmvln2*) were identified and used for phenotypic identification. Finally, four pairs of near-isogenic lines for *ZmVLN2* were obtained and used for comparison of the PVB-related traits of the *Zmvln2* and WT plants. The *Zmvln2* and WT plants were grown in Yuanyang in June 2020. The genotype of the mutant *Zmvln2* was determined via PCR. The primers for amplifying the full-length *ZmVLN2* sequence are listed in Table S11. The PCR program was as follows: 95 °C for 3 min; 34 cycles of 95 °C for 15 s, 58 °C for 20 s, and 72 °C for 20 s; 72 °C for 5 min.

Acknowledgements

We thank the research group of Prof. Jianbing Yan at Huazhong Agricultural University for providing the maize inbred lines and genotypic data. This research was supported by the National Key Research and Development Program of China (2021YFF1000300), the National Natural Science Foundation of China (32171980 and 31971961), the Project funded by China Postdoctoral Science Foundation (2020M682295), the Henan Province Science and Technology Attack Project (202102110012 and 212102110061), the Henan Provincial Higher Education Key Research Project (20A210003), and the Henan Agricultural University Science and Technology Innovation Fund (KJCX2019A01).

Conflicts of interest

The authors declare that they have no conflicts of interest.

Author contributions

J.T. and X.Z. conceived the study. J.T., X.Z., and Y.H. supervised the study. G.S., H.D., J.G., N.L., P.S., H.X., W.L., and Z.F. performed the experiments. G.S. and X.Z. analyzed the data. G.S., X.Z., and J.T. prepared the manuscript. All authors reviewed the manuscript.

References

Atmodjo, M.A., Sakuragi, Y., Zhu, X., Burrell, A.J., Mohanty, S.S., Atwood, J.A. III, Orlando, R. *et al.* (2011) Galacturonosyltransferase (GAUT)1 and GAUT7 are the core of a plant cell wall pectin biosynthetic homogalacturonan: galacturonosyltransferase complex. *Proc. Natl Acad. Sci. USA*, **108**, 20225–20230.

Bao, C., Wang, J., Zhang, R., Zhang, B., Zhang, H., Zhou, Y. and Huang, S. (2012) Arabidopsis *VILLIN2* and *VILLIN3* act redundantly in sclerenchyma development via bundling of actin filaments. *Plant J.* **71**, 962–975.

Barrett, J.C. (2009) Haploview: visualization and analysis of SNP genotype data. *Cold Spring Harb. Protoc.*, **4**, 10.

Borrás, L., Slafer, G.A. and Otegui, M.E. (2004) Seed dry weight response to source–sink manipulations in wheat, maize and soybean: a quantitative reappraisal. *Field. Crop. Res.* **86**, 131–146.

Borrás, L., Westgate, M.E. and Otegui, M.E. (2003) Control of kernel weight and kernel water relations by post-flowering source-sink ratio in maize. *Ann. Bot.* **91**, 857–867.

Bradbury, P.J., Zhang, Z., Kroon, D.E., Casstevens, T.M., Ramdoss, Y. and Buckler, E.S. (2007) TASSEL: software for association mapping of complex traits in diverse samples. *Bioinformatics*, **23**, 2633–2635.

Brown, P.J., Upadyayula, N., Mahone, G.S., Tian, F., Bradbury, P.J., Myles, S., Holland, J.B. *et al.* (2011) Distinct genetic architectures for male and female inflorescence traits of maize. *PLoS Genet.* **7**, e1002383.

Caffall, K.H., Pattathil, S., Phillips, S.E., Hahn, M.G. and Mohnen, D. (2009) *Arabidopsis thaliana* T-DNA mutants implicate *GAUT* genes in the biosynthesis of pectin and xylan in cell walls and seed testa. *Mol. Plant*, **2**, 1000–1014.

Campbell, L., Etchells, J.P., Cooper, M., Kumar, M. and Turner, S.R. (2018) An essential role for abscisic acid in the regulation of xylem fibre differentiation. *Development*, **145**, dev161992.

Chang, T.G. and Zhu, X.G. (2017) Source-sink interaction: a century old concept under the light of modern molecular systems biology. *J. Exp. Bot.* **68**, 4417–4431.

Dettmer, J., Elo, A. and Helariutta, Y. (2009) Hormone interactions during vascular development. *Plant Mol. Biol.* **69**, 347–360.

Endo, S., Iwai, Y. and Fukuda, H. (2019) Cargo-dependent and cell wall-associated xylem transport in *Arabidopsis*. *New Phytol.* **222**, 159–170.

Etchells, J.P., Provost, C.M. and Turner, S.R. (2012) Plant vascular cell division is maintained by an interaction between PXY and ethylene signalling. *PLoS Genet.* **8**, e1002997.

Evans, B.L.T., Dunstone, R.L., Rawson, H.M. and Williams, R.F. (1970) The phloem of the wheat stem in relation to requirements for assimilate by the ear. *Aust. J. Biol. Sci.*, **23**, 743–752.

Franks, P. and Brodribb, T.J. (2005) 4-Stomatal control and water transport in stems. In *Vascular Transport in Plants*, (Holbrook, N.M. and Zwieniecki, M.A., eds), pp. 69–89. Burlington: Academic Press.

Fu, J., Cheng, Y., Linghu, J., Yang, X., Kang, L., Zhang, Z., Zhang, J. *et al*. (2013) RNA sequencing reveals the complex regulatory network in the maize kernel. *Nat. Commun.* **4**, 2832.

Gabriel, S.B., Schaffner, S.F., Nguyen, H., Moore, J.M., Roy, J., Blumenstiel, B., Higgins, J. *et al*. (2002) The structure of haplotype blocks in the human genome. *Science*, **296**, 2225–2229.

Gambín, B.L., Borrás, L. and Otegui, M.E. (2006) Source–sink relations and kernel weight differences in maize temperate hybrids. *Field. Crop. Res.* **95**, 316–326.

He, J.B., Zhao, X.H., Du, P.Z., Zeng, W., Beahan, C.T., Wang, Y.Q., Li, H.L. *et al*. (2018) KNAT7 positively regulates xylan biosynthesis by directly activating *IRX9* expression in *Arabidopsis*. *J. Integr. Plant Biol.* **60**, 514–528.

Honing, H.S., Kieft, H., Emons, A.M.C. and Ketelaar, T. (2012) Arabidopsis VILLIN2 and VILLIN3 are required for the generation of thick actin filament bundles and for directional organ growth. *Plant Physiol.* **158**, 1426–1438.

Huang, C., Chen, Q., Xu, G., Xu, D., Tian, J. and Tian, F. (2016) Identification and fine mapping of quantitative trait loci for the number of vascular bundle in maize stem. *J. Integr. Plant Biol.* **58**, 81–90.

Knapp, S.J. (1986) Confidence intervals for heritability for two-factor mating design single environment linear models. *Theor. Appl. Genet.* **72**, 587–591.

Lee, C., Teng, Q., Huang, W., Zhong, R. and Ye, Z.H. (2009) The F8H Glycosyltransferase is a functional paralog of FRA8 involved in Glucuronoxylan biosynthesis in *Arabidopsis*. *Plant Cell Physiol.* **50**, 812–827.

Li, H., Peng, Z., Yang, X., Wang, W., Fu, J., Wang, J., Han, Y. *et al*. (2013) Genome-wide association study dissects the genetic architecture of oil biosynthesis in maize kernels. *Nat. Genet.* **45**, 43–50.

Li, M.X., Yeung, J.M., Cherny, S.S. and Sham, P.C. (2012) Evaluating the effective numbers of independent tests and significant *p*-value thresholds in commercial genotyping arrays and public imputation reference datasets. *Hum. Genet.* **131**, 747–756.

Li, Y., Tao, H., Zhang, B., Huang, S. and Wang, P. (2018) Timing of water deficit limits maize kernel setting in association with changes in the source-flow-sink relationship. *Front. Plant Sci.* **9**, 1326.

Lin, J.S., Huang, X.X., Li, Q., Cao, Y., Bao, Y., Meng, X.F., Li, Y.J. *et al*. (2016) UDP-glycosyltransferase 72B1 catalyzes the glucose conjugation of monolignols and is essential for the normal cell wall lignification in *Arabidopsis thaliana*. *Plant J.* **88**, 26–42.

Liu, N., Du, Y., Warburton, M.L., Xiao, Y. and Yan, J. (2021) Phenotypic plasticity contributes to maize adaptation and heterosis. *Mol. Biol. Evol.* **38**, 1262–1275.

Liu, Q., Galli, M., Liu, X., Federici, S., Buck, A., Cody, J., Labra, M. *et al*. (2019) *NEEDLE1* encodes a mitochondria localized ATP-dependent metalloprotease required for thermotolerant maize growth. *Proc. Natl Acad. Sci. USA*, **116**, 19736–19742.

Lucas, W.J., Groover, A., Lichtenberger, R., Furuta, K., Yadav, S.R., Helariutta, Y., He, X.Q. *et al*. (2013) The plant vascular system: evolution, development and functions. *J. Integr. Plant Biol.* **55**, 294–388.

Mitsuda, N., Iwase, A., Yamamoto, H., Yoshida, M., Seki, M., Shinozaki, K. and Ohme-Takagi, M. (2007) NAC transcription factors, NST1 and NST3, are key regulators of the formation of secondary walls in woody tissues of *Arabidopsis*. *Plant Cell*, **19**, 270–280.

Nagata, N., Asami, T. and Yoshida, S. (2001) Brassinazole, an inhibitor of Brassinosteroid biosynthesis, inhibits development of secondary xylem in cress pants (*Lepidium sativum*). *Plant Cell Physiol.* **42**, 1006–1011.

Nátrová, Z. (1991) Anatomical characteristics of the uppermost internode of winter wheat genotypes differing in stem length. *Biol. Plant.* **33**, 491–494.

Paterson, A.H., Damon, S., Hewitt, J.D., Zamir, D., Rabinowitch, H.D., Lincoln, S.E., Lander, E.S. *et al*. (1991) Mendelian factors underlying quantitative traits in tomato: comparison across species, generations, and environments. *Genetics*, **127**, 181–197.

Peterson, D.M., Housley, T.L. and Luk, T.M. (1982) Oat stem vascular size in relation to kernel number and weight. *Crop Sci.* **22**, 274–278.

R Core Team. (2020) *R: A language and environment for statistical computing*. Vienna, Austria: R Foundation for Statistical Computing. https://www.R-project.org/

Ruszala, E.M., Beerling, D.J., Franks, P.J., Chater, C., Casson, S.A., Gray, J.E. and Hetherington, A.M. (2011) Land plants acquired active stomatal control early in their evolutionary history. *Curr. Biol.* **21**, 1030–1035.

Sehr, E.M., Agusti, J., Lehner, R., Farmer, E.E., Schwarz, M. and Greb, T. (2010) Analysis of secondary growth in the Arabidopsis shoot reveals a positive role of jasmonate signalling in cambium formation. *Plant J.* **63**, 811–822.

Shane, M., Mccully, M.E. and Canny, M.J. (2000) The vascular system of maize stems revisited: implications for water transport and xylem safety. *Ann. Bot.* **86**, 245–258.

Smetana, O., Mäkilä, R., Lyu, M., Amiryousefi, A., Rodríguez, F.S., Wu, M.F., Solé-Gil, A. *et al*. (2019) High levels of auxin signaling define the stem-cell organizer of the vascular cambium. *Nature*, **565**, 458–489.

Terao, T., Nagata, K., Morino, K. and Hirose, T. (2010) A gene controlling the number of primary rachis branches also controls the vascular bundle formation and hence is responsible to increase the harvest index and grain yield in rice. *Theor. Appl. Genet.* **120**, 875–893.

Wang, X., Cheng, Z., Zhao, Z., Gan, L., Qin, R., Zhou, K., Ma, W. *et al*. (2016) *BRITTLE SHEATH1* encoding OsCYP96B4 is involved in secondary cell wall formation in rice. *Plant Cell Rep.* **35**, 745–755.

Wang, X., Zhang, R., Shi, Z., Zhang, Y., Sun, X., Ji, Y., Zhao, Y. *et al*. (2019) Multi-omics analysis of the development and fracture resistance for maize internode. *Sci. Rep.* **9**, 8183.

Wang, Y., Xu, Y., Pei, S., Lu, M., Kong, Y., Zhou, G. and Hu, R. (2020) KNAT7 regulates xylan biosynthesis in Arabidopsis seed-coat mucilage. *J. Exp. Bot.* **71**, 4125–4139.

Wessels, B., Seyfferth, C., Escamez, S., Vain, T., Antos, K., Vahala, J., Delhomme, N. *et al*. (2019) An AP2/ERF transcription factor ERF139 coordinates xylem cell expansion and secondary cell wall deposition. *New Phytol.* **224**, 1585–1599.

Wu, S., Xie, Y., Zhang, J., Ren, Y., Zhang, X., Wang, J., Guo, X. *et al*. (2015) *VLN2* regulates plant architecture by affecting microfilament dynamics and polar auxin transport in rice. *Plant Cell*, **27**, 2829–2845.

Xiao, Y., Liu, H., Wu, L., Warburton, M. and Yan, J. (2017) Genome-wide association studies in maize: praise and stargaze. *Mol. Plant*, **10**, 359–374.

Xiao, Y., Tong, H., Yang, X., Xu, S., Pan, Q., Qiao, F., Raihan, M.S. *et al*. (2016) Genome-wide dissection of the maize ear genetic architecture using multiple populations. *New Phytol.* **210**, 1095–1106.

Yamamoto, R., Fujioka, S., Demura, T., Takatsuto, S., Yoshida, S. and Fukuda, H. (2001) Brassinosteroid levels increase drastically prior to morphogenesis of tracheary elements. *Plant Physiol.* **125**, 556–563.

Yang, N., Lu, Y., Yang, X., Huang, J., Zhou, Y., Ali, F., Wen, W. *et al*. (2014) Genome wide association studies using a new nonparametric model reveal the genetic architecture of 17 agronomic traits in an enlarged maize association panel. *PLoS Genet.* **10**, e1004573.

Zhai, L., Zheng, T., Wang, X., Wang, Y., Chen, K., Wang, S., Wang, Y. *et al*. (2018) QTL mapping and candidate gene analysis of peduncle vascular bundle related traits in rice by genome-wide association study. *Rice*, **11**, 13.

Zhang, X., Sun, S., Nie, X., Boutté, Y., Grison, M., Li, P., Kuang, S. *et al*. (2016) Sterol methyl oxidases affect embryo development via auxin-associated mechanisms. *Plant Physiol.* **171**, 468–482.

Zhou, J., Lee, C., Zhong, R. and Ye, Z.H. (2009) MYB58 and MYB63 are transcriptional activators of the lignin biosynthetic pathway during secondary cell wall formation in *Arabidopsis*. *Plant Cell*, **21**, 248–266.

Supporting information

Additional supporting information may be found online in the Supporting Information section at the end of the article.

Table S1 Peduncle vascular bundle-related traits evaluated in this study.
Table S2 Analysis of the variance of 15 traits across three locations in the association panel.
Table S3 All candidate genes within the significant loci identified by a GWAS.
Table S4 Comparison of the genetic effects of haplotypes on PVB-related traits and yield-related traits.
Table S5 Inbred lines classified according to their origin and source in the four haplotype groups.
Table S6 QTL detected by the SLM analysis of ear traits in 10 maize recombinant inbred lines.
Table S7 QTL detected by the JLM analysis of ear traits in 10 maize recombinant inbred lines.
Table S8 QTL detected by a GWAS of ear traits in 10 maize recombinant inbred lines.
Table S9 QTL detected by a GWAS of ear traits in a maize NAM population.
Table S10 Pedigree information or the source of the maize inbred lines used in this study.
Table S11 Primers used in this study.
Figure S1 Frequency distribution of the PVB-related traits of the association mapping population at three locations.
Figure S2 Distribution of the 15 PVB-related traits in the association mapping population.
Figure S3 Manhattan and quantile–quantile plots for 15 PVB-related traits for the association panel at three locations.
Figure S4 Functional annotations of 348 candidate genes identified by a GWAS as significantly associated with 15 PVB-related traits.
Figure S5 Comparison of 15 PVB-related traits among Hap1, Hap2, Hap3, and Hap4 according to an independent *t*-test ($P < 0.001$).
Figure S6 Phenotypic correlation coefficients between the PVB-related traits and yield traits.